Water Supply

IWA PUBLISHING

Water Supply Vol 22 No 1, 220 doi: 10.2166/ws.2021.279

Hydraulic characterization of porous pipes

Yasmin Fernandes Silva [a], Luiz Antonio Lima [a], Michael Silveira Thebaldi [a,*], Virgílio Henrique Barros Nogueira [a], Adriano Valentim Diotto [a] and Julia Fonseca Colombo Andrade [b]

[a] Universidade Federal de Lavras, Department of Water Resources, PO Box 3037, Postal Code 37200-900 Lavras, Minas Gerais, Brazil
[b] Universidade de São Paulo, Escola de Engenharia de São Carlos, Avenida Trabalhador Sãocarlense, 400, Centro. Postal Code 13566-590 São Carlos, São Paulo, Brazil
*Corresponding author. E-mail: michael.thebaldi@ufla.br

YFS, 0000-0002-5508-3427; LAL, 0000-0002-5542-6442; MST, 0000-0002-4579-6714; VHBN, 0000-0002-7143-9454; JFCA, 0000-0001-8496-3258

ABSTRACT

Increased anthropic activity in the environment leads to degradation and increased waste generation that includes tires, which can be used for the manufacture of porous pipes by extrusion for irrigation or aeration. There are no defined methodologies for the hydraulic characterization of porous pipes; in addition, their performance is questionable because the permeability of the wall in contact with water seems to decrease with time. Thus, this study aimed to perform the hydraulic characterization of porous pipes. Experiments were performed to assess the variation in permeability over time, the head loss, the friction factor, and the roughness. Statistical tests were performed to investigate possible significant differences between treatments. The results showed that the permeability varies over time and tends to decrease with each application of water. After a certain period, the permeability tends to become constant, and a stable flux can be determined, being the lowest average permeability and flux values found 0.591×10^{-15} m^2 0.109 m^3·m^{-2}·s^{-1}. There is variability in the permeability between pipe samples from the same batch as well as variability within the same sample, as indicated by the fact that some samples are similar to each other while others differ when performing a pairwise multiple comparison.

Key words: friction factor, permeability, pipe wall roughness, trickle irrigation

HIGHLIGHTS

- Permeability over time, head loss, friction factor and roughness of porous pipes were evaluated.
- Variations in intrinsic permeability and flow depend on the service pressure.
- The variation of permeability over time decreases with each water application.
- Permeability stabilizes after some time, allowing the determination of a stable flow.
- Stable flow can be used to determine when the water application becomes steady.

INTRODUCTION

Due to environmental and public health concerns, sustainable methods for proper waste disposal are being discussed. The final disposal of waste tires causes problems because when improperly performed, it has several negative effects on the environment (Kowalska *et al.* 2002; Sant'anna *et al.* 2015).

Waste tires may be used as raw materials to produce porous irrigation pipes. Commercially marketed as porous soaker hoses and immersion tubes, their use and application are more common in arid and semiarid regions. The advantages of their use for irrigation include their flexibility and use under low pressure, consequently leading to low operational costs (Alam 1995; Janani *et al.* 2011).

Porous pipes are ideal for trickle irrigation because they are easy to install in specific locations to directly apply water to an area of interest and because they are flexible, and the functionality of these pipes is related to the way the water is transported and emitted. In irrigation, these pipes are categorized as a linear emission source; that is, a source in which water is distributed along the entire length and forms a continuous wetting front. However, studies have shown that the permeability of these pipes varies over time, negatively affecting their use in irrigation (Teeluck & Sutton 1998; Rettore *et al.* 2014; Kanda *et al.*

2018). Considering the variation in permeability over time, the performance of a surface application system may be negatively impacted since the amount of water applied is inconstant (Fang *et al.* 2000; Kang 2000; Shu *et al.* 2007; Ren *et al.* 2017).

The variation in the permeability of flexible porous pipes, which affects the water emission characteristics, may be a consequence of the pressure used, and an increase in flow rate is directly proportional to an increase in pressure. The water quality also affects their application since suspended solids and microorganisms present in the water can clog the micropores of the pipeline, leading to irregular water distribution; however, non-permanent water application tends to result in stabilization (Tripathi *et al.* 2011; Lyu *et al.* 2016; Zhang *et al.* 2017).

To ensure the proper use of porous pipes in irrigation, it is necessary to know the hydraulic characteristics to evaluate the variation in the flow rate over time. In addition, the technical information of the product, such as how the flow rate varies with pressure, needs to be defined. In this context, the objective in this work is to perform the hydraulic characterization of porous pipes used in irrigation regarding the variation in their permeability over time relative to the operating pressure, as well as to evaluate the head loss in these pipes, specifically to determine their friction factor and roughness.

METHODS

Permeability of porous pipes

A hydraulic apparatus was used to evaluate the permeability of porous pipes, which enabled the determination of the flow rate variation through pipe segments over time with different pressure values at the inlet of the pipes. Three pipe samples measuring 0.20 m in length, 0.011 m in internal diameter, and 0.018 m in external diameter were used. The annular volume of the pipes was calculated by using the pipe cross-sectional area and the pipe length. The annular volume obtained was 0.0000319 m^3. The surface area of the pipes' length was 0.01131 m^2.

The system used consisted of a compressor with a pressure regulator connected to a Mariotte bottle that was built with a PVC pipe with a nominal pressure of 8,000 kPa, measured to be 1.08 m high and 0.3 m in diameter. The bottle was connected to a calibrated load cell with a capacity of 100 kg ($\pm$ 0.02 kg). The load cell and the Mariotte bottle were suspended on a tripod (Figure 1).

A pipe segment was connected to the Mariotte bottle using a valve; the inlet pressure was measured via a pressure transducer connected to the porous pipe. This pipeline was located 0.10 m above the bottom of the bottle and was placed over a container to allow part of the applied water to be collected in the container for temperature measurement.

The load cell, the thermometer, and the pipeline where the pressure was measured were connected to a Campbell Scientific® data logger, model CR10. The mean flow rate was calculated using the difference in water volume in the Mariotte bottle before and after application. With the mean flow rate, the mean flux through the pipeline could be calculated using the ratio between the average flow rate and the mean flow rate between the external and internal areas of the porous pipe.

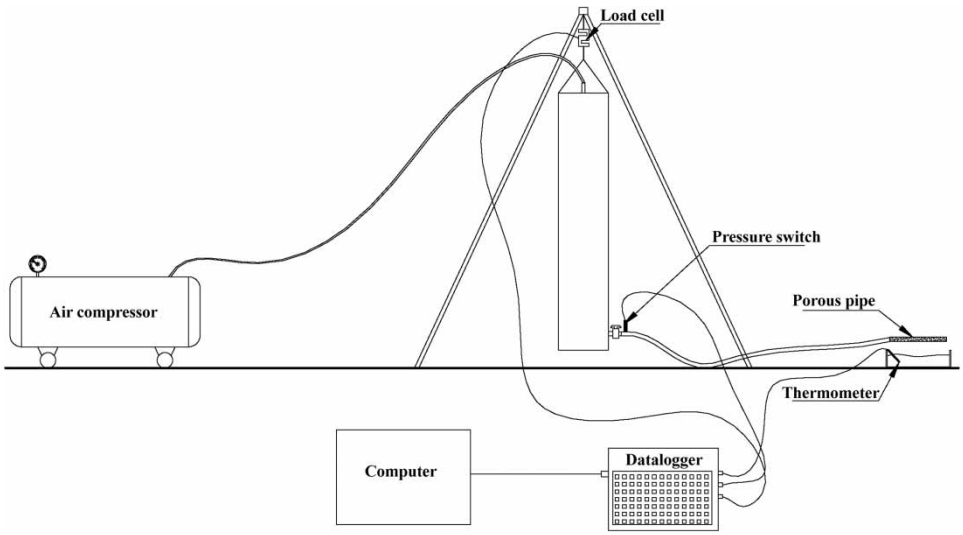

Figure 1 | Representation of the experimental apparatus with the components used.

To evaluate the repeatability of the experiment, the porous pipes were weighed to determine if mass loss occurred after use; since the pipes are made of agglomerated microscopic rubber particles, their mass decreased due to the loss of material particles when they were subjected to a certain pressure. Thus, prior to the performance of each test, the pipes were weighed. Immediately after their use, the pipe samples were dried in a forced-air oven at 40 °C to eliminate residual moisture; this temperature was selected to prevent damage to the material. The water flux (Equation (1)) was calculated by using the mean flow rate obtained by taking the difference between the initial and final water volumes at the time of collection:

$$q = \frac{Q_{mean}}{S_S} \tag{1}$$

where q is the water flux through the porous pipes ($m^3\ m^{-2}\ s^{-1}$), Q_{mean} is the mean flow rate ($m^3\ s^{-1}$), and S_S is the surface area (m^2).

With the values of the water flux through each porous pipe, Darcy's law (Equation (2)) was used to determine the hydraulic conductivity. Thus, the permeability of each pipe could be calculated (Equation (3)):

$$q = -k_0 \times \frac{dH}{dx} \tag{2}$$

where k_0 is the saturated hydraulic conductivity of the porous pipes ($m\ s^{-1}$) and dH/dx is the hydraulic head gradient ($m\ m^{-1}$). Note that the hydraulic conductivity can be calculated as:

$$k_0 = \frac{k \times g \times \rho}{\mu} \tag{3}$$

where k is the intrinsic permeability of the porous pipes (m^2), μ is the dynamic viscosity of the fluid ($Ns\ m^{-2}$), and g is the gravitational acceleration (considered to be $9.81\ m\ s^{-2}$).

A thermometer was used to record the temperature in the studied intervals, and then the mean and standard deviation were obtained for each pressure studied and for each irrigation performed (Table 1). The kinematic viscosity was calculated using the equation presented by Azevedo Netto & Fernandez y Fernandez (2015).

The volumetric moisture of the porous pipe segments was obtained from the ratio between the final and initial mass of the material with respect to the annular volume and the specific mass of the water. The variation in the moisture present in the pipes assuming that the water density was $1{,}000\ kg\ m^{-3}$ is shown in Table 2.

Data were collected for 300 minutes, and pressures of 50, 75, and 150 kPa were evaluated; these values were within the range of pressures tested by other authors for the same type of material (Lomax *et al.* 1986, 1988; Mohammad 1998; Teeluck & Sutton 1998).

Due to the stability of the water flux through the porous pipes, the observed water flux data as a function of time were fitted to the derivative of the Kostiakov mathematical model (Kostiakov 1932) of soil water infiltration (Equation (4)) due to the

Table 1 | Temperature and kinematic viscosity obtained for each pressure value in each replication

	Temperature (°C)		Kinematic viscosity ($m^2\ s^{-1}$)	
Pressure (kPa)	Mean	Standard deviation (±)	Mean × (10^{-7})	Standard deviation (±) × (10^{-8})
50	24.844	0.531	8.99	1.10
	23.882	0.913	9.19	1.96
	26.104	0.589	8.73	1.17
75	23.953	0.580	9.17	1.24
	23.850	0.578	9.20	1.24
	21.034	0.594	9.83	1.42
150	25.655	0.407	8.82	8.19
	22.666	0.421	9.46	9.44
	22.913	0.603	9.40	1.34

Table 2 | Variation in the moisture present in the porous pipes after drying

Pressure (kPa)	Test	Moisture (m^3 of water per m^3 of material)
50	1	0.0242
	2	0.0263
	3	0.0461
75	1	0.0100
	2	0.0160
	3	0.0179
150	1	0.0154
	2	0.0210
	3	0.0223

similarities in the behaviour observed. It was assumed that the water flux through the porous pipe wall is analogous to the water flux upon entering the soil surface (infiltration):

$$q = \alpha \times \beta \times t^{\beta-1} \tag{4}$$

where q is the flux density ($m^3\ m^{-2}\ s^{-1}$), t is the time considered (s^{-1}), and α and β are empirical parameters of the Kostiakov model.

To determine the expected stable flux for the fitted curves, the moment at which the variation in the flux as a function of time – determined by Equation (4) – becomes minimal; that is, the stability of the flux with time, was considered. For this purpose, Equation (5) was used considering the empirical parameters fitted in each test. Note that the flux is stable for each test but may be modified if there are any changes in the physical conformation of the porous pipes.

$$q_{stable} = \alpha \times \left(\frac{-0.001}{\beta \times \alpha}\right)^{\frac{\beta}{\beta-1}} \tag{5}$$

Here, q_{stable} is the stable flux ($m^3\ m^{-2}\ s^{-1}$).

For the evaluation of the water flux and permeability of porous pipes due to a sequence of use events, a 3×3 factorial completely randomized design (CRD) was considered with 30 replications in time, with the inlet pressure of the porous pipes (three levels: 50, 75, and 150 kPa) and cumulative sequence of tests (three levels: one, two, and three tests) as sources of variation. Analysis of variance was performed by applying the F test at 5% statistical probability; when significant differences were found between treatments, Tukey's test was used at 5% statistical probability.

For the analysis of the stable flux and determination of the fitting parameters of mathematical models representative of the water flux through porous pipes, a CRD with three replications and one source of variation – the inlet pressure in porous pipes, with three levels (50, 75, and 150 kPa) – was considered. Analysis of variance was also performed by applying the F test at 5% statistical probability, and if significant differences were found between treatments, Tukey's test was also used at 5% probability.

Hydraulic head loss and absolute roughness

For this evaluation, a 5.5 m porous pipe segment was externally sealed and enveloped in a PVC pipe 0.022 m in diameter; the PVC pipe was closed at both ends and completely filled with water. As a result, there was no flux through the pipe wall pores, and thus the pipe began to behave as a stream tube; that is, with an impermeable wall. The system was assembled by placing a one-metre-high reservoir on an elevated surface 8.4 m above the axis of the porous piping tested. In the reservoir, a pipe responsible for supplying water to the porous pipe was connected, and a ball valve was placed in front of the pipe inlet to control the water outflow. The constant water head in the upper reservoir was monitored by observing the water flux through a spillway located in the upper reservoir. The porous pipe was positioned horizontally and subjected to the hydrostatic pressure of a 9.4 m water column. A schematic representation of the assembled apparatus is shown in Figure 2.

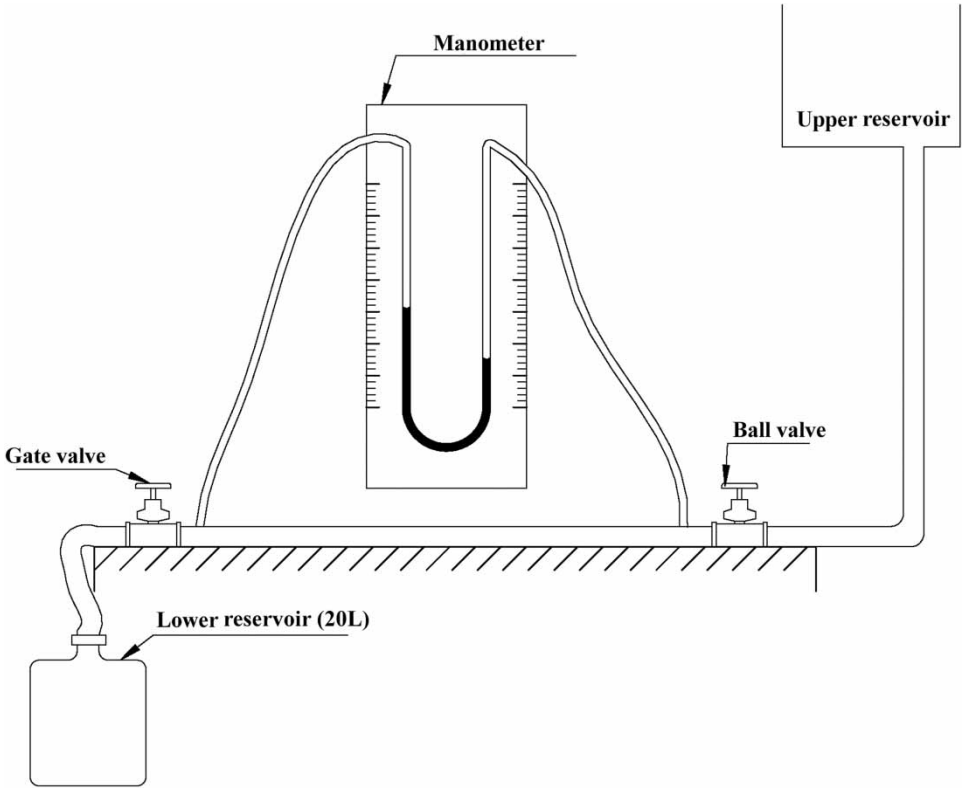

Figure 2 | Simplified representation of the apparatus built to determine the head loss in porous pipe segments made from rubber tires.

The first branch of the differential manometer was connected through a pressure gauge located 1.25 m after the initial valve at a distance equivalent to 69.44 diameters from the porous pipe to ensure full development and stabilization of the flux. The second branch of the differential manometer was connected 1.25 m downstream from the valve of the apparatus for control and variation of the flow rate. The flow rate was measured by weighing the water in the lower reservoir after collecting it for one minute. The measurement of the flow rate and reading of the pressure difference in the porous pipe segment were performed only after a steady-state flow was observed.

To obtain the pressure values, a mercury U-tube manometer was used. The experiment was performed using four samples of porous pipes under five different flow rates. Thus, the head loss was calculated by using the pressure difference measured in each porous pipe segment. The Reynolds number was calculated using Equation (6), and the friction factor, f, was obtained using the Darcy-Weisbach head loss equation (Equation (7)). With the f value observed in each test, the roughness of the pipes could be approximated using the Swamee-Jain formula (Equation (8)).

$$\mathrm{Re} = \frac{VD}{\upsilon} \tag{6}$$

Here, Re is the Reynolds number (dimensionless), V is the mean flow velocity (m s^{-1}), D is the internal diameter of the porous pipe (m), and υ is the kinematic viscosity of the water (m^2 $s-1$).

$$hf = f \times \frac{L}{D} \times \frac{v^2}{2g} \tag{7}$$

Here, hf is the major head loss (m), f is the friction factor (dimensionless), and L is the length of the porous pipe tested (m).

$$f = \frac{0.25}{\left[\log\log\left(\frac{\varepsilon}{3.7D} + \frac{5.74}{Re^{0.9}}\right)\right]^2} \quad (8)$$

Here, ε is the roughness of the porous pipe tested (m).

The values obtained for the absolute roughness and friction factor in each porous pipe were initially compared using descriptive statistics with boxplots. In addition, mathematical models were fitted to determine the trend of the data relative to the Re values observed for each of the samples evaluated.

The Kruskal-Wallis H test, also called the one-way ANOVA on ranks, was used with a significance level of 5% to identify possible significant differences between the roughness and friction factor obtained for the evaluated porous pipe samples. Once significant differences between samples were detected for the analysed response variable, a pairwise multiple comparison was performed using Tukey's test at 5% statistical probability.

RESULTS AND DISCUSSION

Flux and permeability through the porous pipe wall

A summary of the analyses of variance of the flux and permeability is shown in Table 3. The simple effects of the pressure and of the test for the water flux through the porous pipe and its permeability were significant at the 1% level. In addition, the effect of the interaction between the two sources of variation on the abovementioned response variables was significant.

According to Table 4, the permeability values obtained by Tukey's test for pressures of 50 and 150 kPa were equal at the 1% probability level. Separate analyses of the tests showed differences, and the permeability decreased with increasing test number, which supports the idea that the permeability decreases with use. The tests showed the usability of the pipes with time, and even after drying, there was a difference between the flux and permeability data.

As shown in Table 4, an increase in permeability was observed due to an increase in pressure from 50 kPa to 75 kPa, thus indicating a probable expansion of the pore space of the material. However, regarding the difference in the permeability values at 75 and 150 kPa, as the pressure increased, the pore space may have also decreased due to the effects of pressure,

Table 3 | Analysis of variance of the flux and permeability with increasing pressure and for the test performed

		F	
Source of variation	**Degrees of Freedom**	**q ($m^3\ m^{-2}\ s^{-1}$)**	**k $\times 10^{-16}$ (m^2)**
Pressure (P)	2	201.26**	36.07**
Test (T)	2	119.66**	71.77**
P × T	4	19.06**	3.13*
Error	261		
Total	269		

**Significant at the 1% probability level ($p < 0.01$); *significant at the 5% probability level ($p < 0.05$).

Table 4 | Simple effects of the service pressure and sequence of tests on the intrinsic permeability of the studied porous pipes

Pressure (kPa)	**k (m^2) $\times 10^{-15}$**	**Test**	**k (m^2) $\times 10^{-15}$**
50	0.877 b	1	1.192 a
75	1.123 a	2	0.889 b
150	0.785 b	3	0.704 c

Values followed by the same letter in the columns do not differ according to Tukey's test at the 1% significance level.

leading to a reduction in the permeability. Thus, the granules that formed the porous pipes physically changed according to the variation in pressure; the pore space decreased for some pressure values and increased for others.

The manufacture of porous pipes results in pipes with nonuniform positions and pore sizes, which leads to variations in the application of water when these pipes are used for irrigation. According to the analysis of variation from one manufactured batch to another, there is variation both within the same batch and between different batches (Teeluck & Sutton 1998).

Janani *et al.* (2011) evaluated the pressure variation and its impact on the water distribution of porous pipes made from recycled tires. The results obtained in their study were similar to those of the present study in that the service pressure affected the water application, with the pressure discharge exponent being greater than 1. The cited authors also determined that the uniformity in the application of water varied with the pressure and that there was a drastic reduction in the flux at the beginning, with a steady-state flux being reached after a certain time. These authors also found a change in the microstructure of porous pipes.

Table 5 shows that in the first and third tests, the values obtained at pressures of 50 and 150 kPa did not show significant differences at the 5% probability level according to Tukey's test; the value found for a pressure of 75 kPa was higher than those of the other pressures. In the second test, significant differences were observed among all the pressure levels considered. Comparing the variations in pressure for each pressure level in the different tests, under 50 kPa of pressure and in the first two tests, the values did not differ. At 75 kPa, all the tests differed from each other, with significant differences being observed. In addition, the fact that the values were higher than those found for the 150 kPa case suggested the irregular modification of the pipe due to the pressure effect. Conversely, for 150 kPa, the data of the second and third tests were statistically similar.

Figure 3 shows the variation in permeability as a function of time for different pressures and tests. At a pressure of 50 kPa (Figure 3(a)), the permeability values decreased with time, and the permeability variability decreased after a certain amount of time; that is, approximately 150 minutes. For test 3, the variation in the data became stable earlier than in the other tests; that is, the variability in the permeability decreased with time as the pipe was sequentially used.

The permeability variabilities for pressures of 75 and 150 kPa were similar, with the values decreasing with time and for different tests. The curves of the second and third tests were close at a pressure of 150 kPa, which showed that there was instability when the pressure increased.

Table 6 shows the mathematical models obtained for permeability relative to time at pressures of 50, 75, and 150 kPa, and Table 7 presents the behavioural permeability mathematical models as a function of time for the first, second, and third cumulative tests. Figure 4 shows that the variation in the permeability with pressure is inconstant since the permeability does not increase with increasing pressure, unlike the trend observed for the flux values in Figure 3. As shown in Figure 4(a), where the plotted data refer to the first test, the permeability values for 75 kPa were greater than those for 150 kPa (Table 5), and the values for 150 kPa were greater than those for 50 kPa. However, for tests 2 and 3, the permeability values for 50 kPa were higher than those for 150 kPa.

Figure 4(b) and 4(c) (tests 2 and 3) show a slight variation in the permeability data as a function of time, with a linear trend over a shorter time interval. For pressures of 50 and 75 kPa in the evaluated tests, this did not occur so quickly.

As previously mentioned, during the manufacturing process, porous pipes undergo grinding and then are shaped by an extruder. Thus, when the small rubber particles come together, they form small pores, which is a possible explanation for the reduction in permeability over time. When the pipe walls are subjected to pressurized flow, the size of these pores may decrease because of wall compaction, leading to the partial obstruction of some pores and thus decreasing the flow

Table 5 | Intrinsic permeability of the porous pipes, evaluated under different service pressures and test sequences

	Permeability $\times 10^{-15}$ (m²)		
	Tests		
Pressure (kPa)	1	2	3
50	1.045 b A	0.909 b A	0.677 b B
75	1.423 a A	1.192 a B	0.845 a C
150	1.109 b A	0.655 c B	0.591 b B

Values followed by the same lowercase letter in columns and uppercase letters in rows do not differ from each other according to Tukey's test at the 5% significance level.

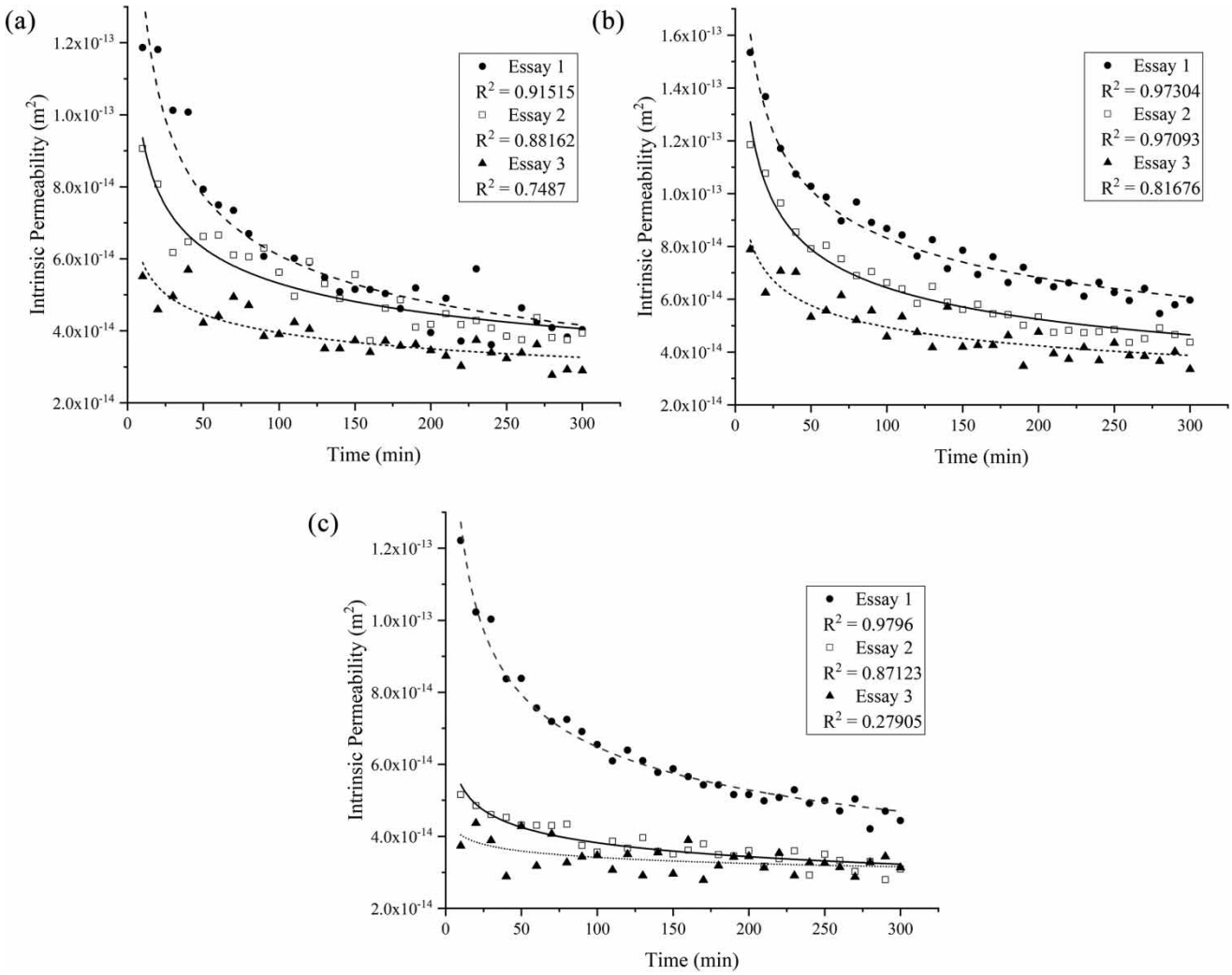

Figure 3 | Permeability as a function of time for the tests at pressures of 50 (a), 75 (b), and 150 (c) kPa.

Table 6 | Mathematical models of permeability as a function of time for the tests at pressures of 50, 75, and 150 kPa

Pressure	Test 1	Test 2	Test 3
50 kPa	$k = (3.03468.10^{-13}).t^{-0.34851}$	$k = (1.64841.10^{-13}).t^{-0.24569}$	$k = (8.80242.10^{-14}).t^{-0.17398}$
75 kPa	$k = (3.09058.10^{-13}).t^{-0.28508}$	$k = (2.51296.10^{-13}).t^{-0.29571}$	$k = (1.3742.10^{-13}).t^{-0.22203}$
150 kPa	$k = (2.4983.10^{-13}).t^{-0.29309}$	$k = (4.7730710^{-14}).t^{-0.07263}$	$k = (4.77307.10^{-14}).t^{-0.07263}$

Table 7 | Mathematical models of permeability as a function of time for the first, second, and third cumulative tests at pressures of 50, 75, and 150 kPa

Test	50 kPa	75 kPa	150 kPa
1	$k = (3.03468.10^{-13}).t^{-0.34851}$	$k = 3.09058.10^{-13}.t^{-0.28508}$	$k = (2.4983.10^{-13}).t^{-0.29309}$
2	$k = (1.64841.10^{-13}).t^{-0.24569}$	$k = 2.51296.10^{-13}.t^{-0.29571}$	$k = (7.75736.10^{-14}).t^{-0.15374}$
3	$k = (8.80242.10^{-14}).t^{-0.17398}$	$k = 1.3742.10^{-13}.t^{-0.22203}$	$k = (4.77307.10^{-14}).t^{-0.07263}$

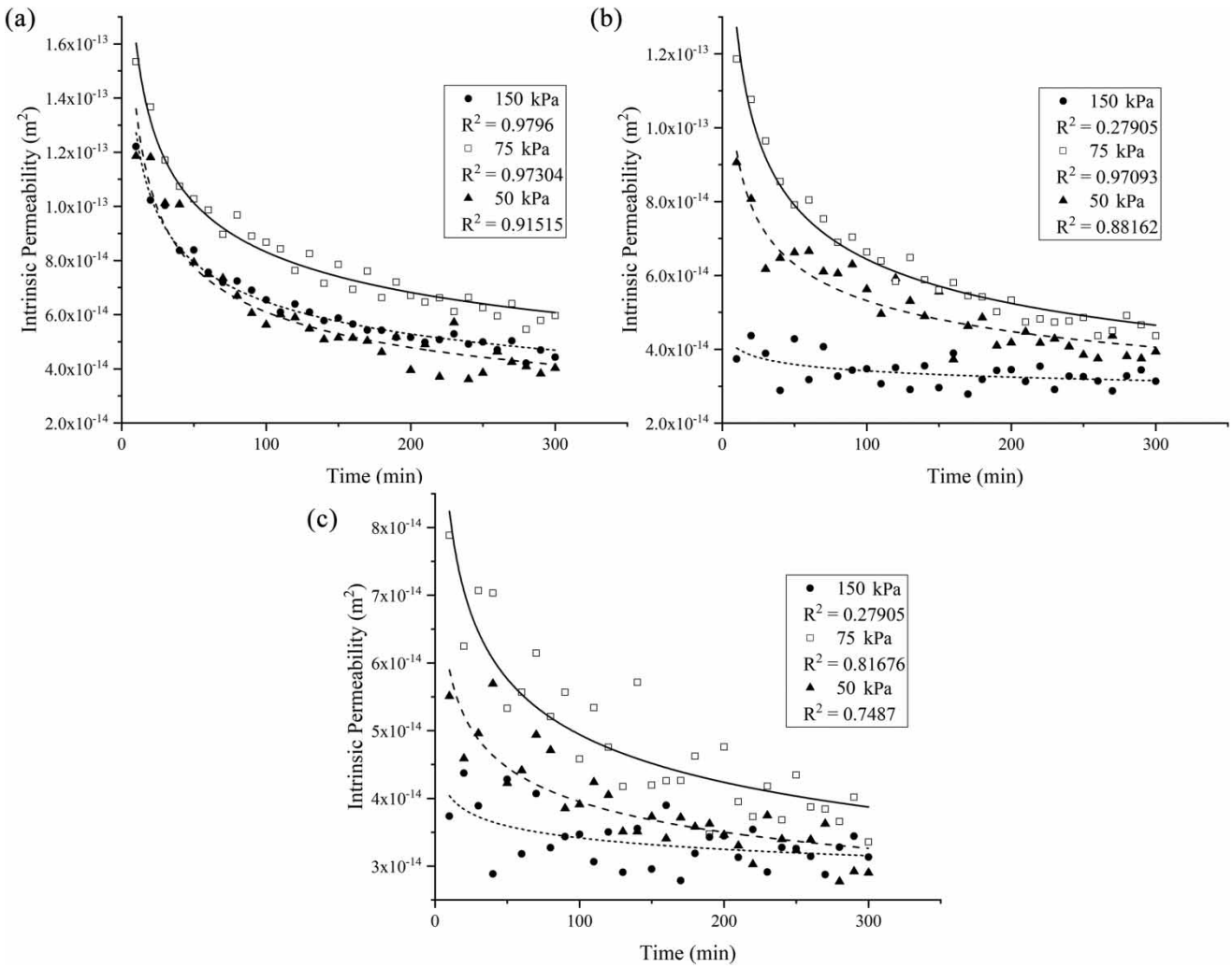

Figure 4 | Variation in permeability as a function of time for the first (a), second (b), and third (c) cumulative tests at pressures of 50, 75, and 150 kPa.

rate over time due to the reduced diameter and, consequently, pipe volume (Bradley *et al.* 2001; Casimiro 2011; Shahzad *et al.* 2015).

The results of a study using porous ceramic emitters buried in two types of soil (Cai *et al.* 2018) were similar to those found in this study: the flow rate of the emitter dropped rapidly at the beginning of the test and then gradually decreased until it reached a stable value.

A simple comparison between the pressures and tests presented in Table 8 shows that the fluxes among service pressures differed from each other at the 1% probability level; however, unlike the permeability, the values of which did not follow a

Table 8 | Simple effect of the inlet pressure and cumulative irrigation tests on the water flux through the porous pipes

Pressure (kPa)	q ($m^3\ m^{-2}\ s^{-1}$)	Test	q ($m^3\ m^{-2}\ s^{-1}$)
50	0.143 c	1	0.348 a
75	0.259 b	2	0.229 b
150	0.361 a	3	0.186 c

Values followed by the same letter in the columns do not differ according to Tukey's test at the 1% significance level.

trend, the flux increased with increasing pressure. From analyses of the different tests, data consistency was again observed, with a decrease in the flux values as the number of tests increased, corroborating with the decrease in permeability over time.

Regarding the effects on the flux during the use of porous pipes, the flux variations in test 1 were significantly different according to Tukey's test for all pressures analysed (Table 9). For test 2, the flux values at 75 and 150 kPa were statistically equal at 1% probability. The analysis of test 3 showed a difference between the fluxes for the pressures evaluated. The results presented in Table 9 show a flux increase with increasing pressure for the three analysed tests.

In the evaluation of the variation among tests, from an analysis of the plotted curves for each pressure, a difference was noted between the first test and the other tests at 50 kPa, but the values for tests 2 and 3 did not differ. At 75 kPa, there were differences between the calculated flux values in the three tests analysed. The behaviour at a pressure of 150 kPa was similar to that observed at 50 kPa because only tests 2 and 3 were similar. The same trend was observed for the flux values relative to the number of tests for each pressure level; that is, there was a decrease in flux with increased use of the porous pipes. Additionally, the flux tended to increase with increasing pressure within each test.

Table 10 shows that only the stable flux presented significantly different values according to the F test at 5% probability, with the empirical parameters of the Kostiakov model being statistically equal for all analysed inlet service pressures.

Table 11 shows that there were similarities between the values of q_{stable} at a pressure of 75 kPa relative to those observed for pressures of 50 and 150 kPa; however, the latter two differed from each other. As already presented, there were no differences among the empirical parameters of the Kostiakov model with pressure variation.

Figure 5(a) shows the flow variation with the test time for a pressure of 50 kPa. In the three replications, the curves had a steep slope from 0 minutes to 50 minutes, after which the curves tended to stabilize with time as the flux decreased with use; that is, the test time.

With increasing pressure, the curves for tests 2 and 3 tended to deviate from the curve for test 1, and this was more evident for a pressure of 150 kPa. From the analyses at this pressure (Figure 6), the corresponding curve tended to exhibit linear behaviour earlier than the curves at 50 and 75 kPa.

After 150 minutes, replications 2 and 3 – performed after drying – practically overlapped (Figure 5(c)). Rettore Neto *et al.* (2014) identified that porous pipes are subjected to changes in diameter due to internal pressure because they are elastic; this explains the variation among the curves obtained under different pressures. Wałowski (2017) studied the variation in the gas

Table 9 | Effect of the interaction between the inlet pressure and the cumulative irrigation tests on the water flux through the porous pipes

	Flux ($m^3\ m^{-2}\ s^{-1}$)		
	Tests		
Pressure (kPa)	1	2	3
50	0.184 c A	0.136 b B	0.109 c B
75	0.334 b A	0.260 a B	0.183 b C
150	0.526 a A	0.290 a B	0.266 a B

Values followed by the same lowercase letter in columns and uppercase letters in rows do not differ from each other according to Tukey's test at the 5% significance level.

Table 10 | Analysis of variance of the effect of pressure on variations in the stable flux, where α and β are empirical parameters of the Kostiakov model

		F		
Source of variation	Degrees of Freedom	q_{stable}	α	β
Pressure (kPa)	2	7.20*	0.61^{NS}	1.36^{NS}
Error	6			
Total	8			

*Significant at the 5% probability level according to the F test ($p < 0.05$); NS: not significant ($p \geq 0.05$).

Table 11 | Simple effect of the service pressure on the values of the stable flux and the empirical parameters of the Kostiakov model adapted to the performed tests

Pressure (kPa)	q_{stable} ($m^3\ m^{-2}\ s^{-1}$)	α	β
50	0.176 b	0.496 a	− 0.249 a
75	0.282 ab	0.912 a	− 0.258 a
150	0.395 a	0.963 a	− 0.161 a

Values followed by the same letter in the columns do not differ from each other according to Tukey's test at the 5% significance level.

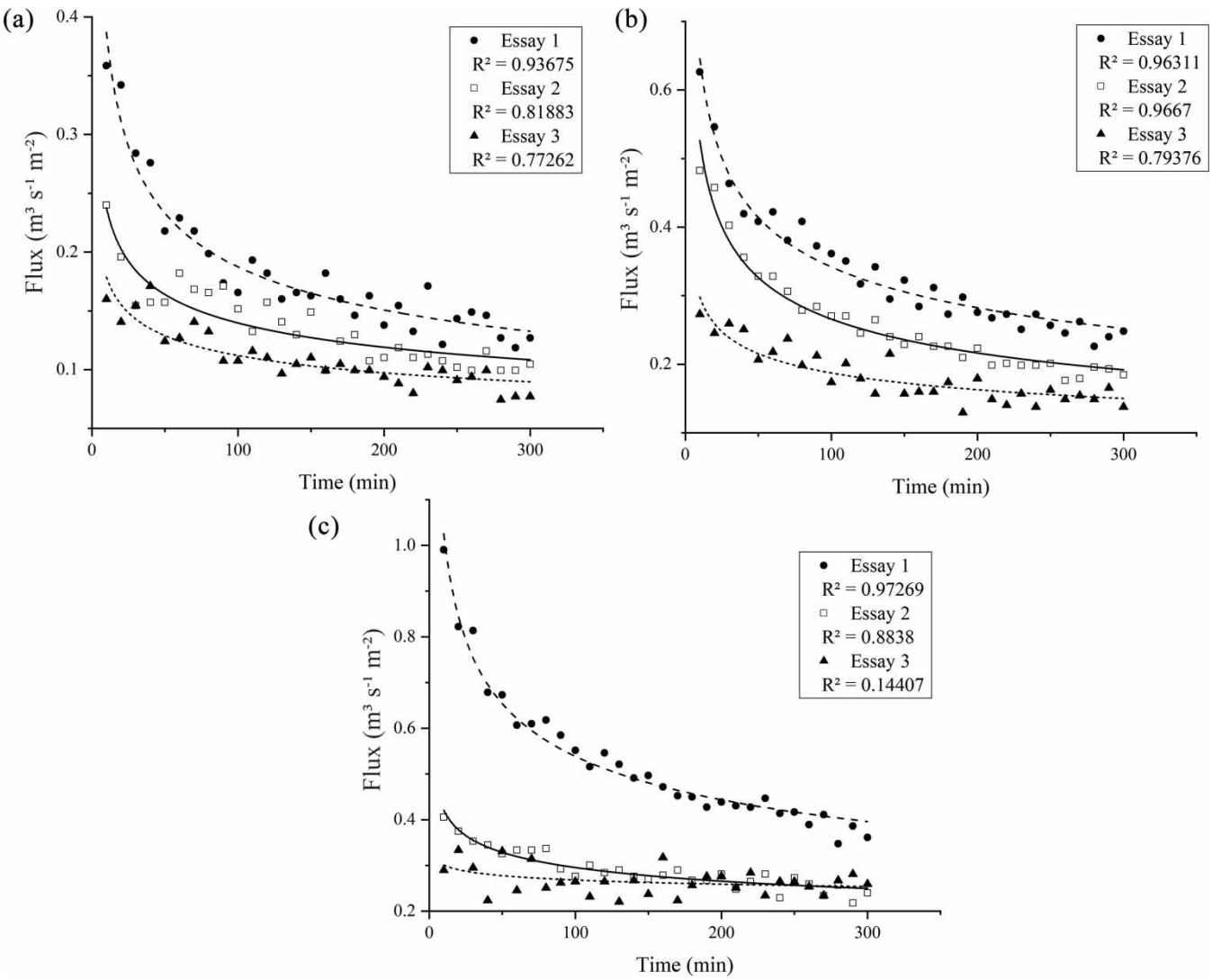

Figure 5 | Flux in porous pipes as a function of time for the tests at pressures of 50 (a), 75 (b), and 150 (c) kPa.

permeability coefficient in porous materials and observed that the flow rate decreases with decreasing pressure. Even with differences between the studied fluids, the results obtained by that author corroborate those observed in this study; that is, transient flux behaviour was observed with changing material properties.

Figure 5 shows that the R^2 values were high for pressures of 50 and 75 kPa, which shows that the fitted models can accurately explain the observed values. However, for the case of 150 kPa in the last test, the R^2 value was 0.144, which is low and shows that the model is not able to fully explain the data variability despite the obtained significance.

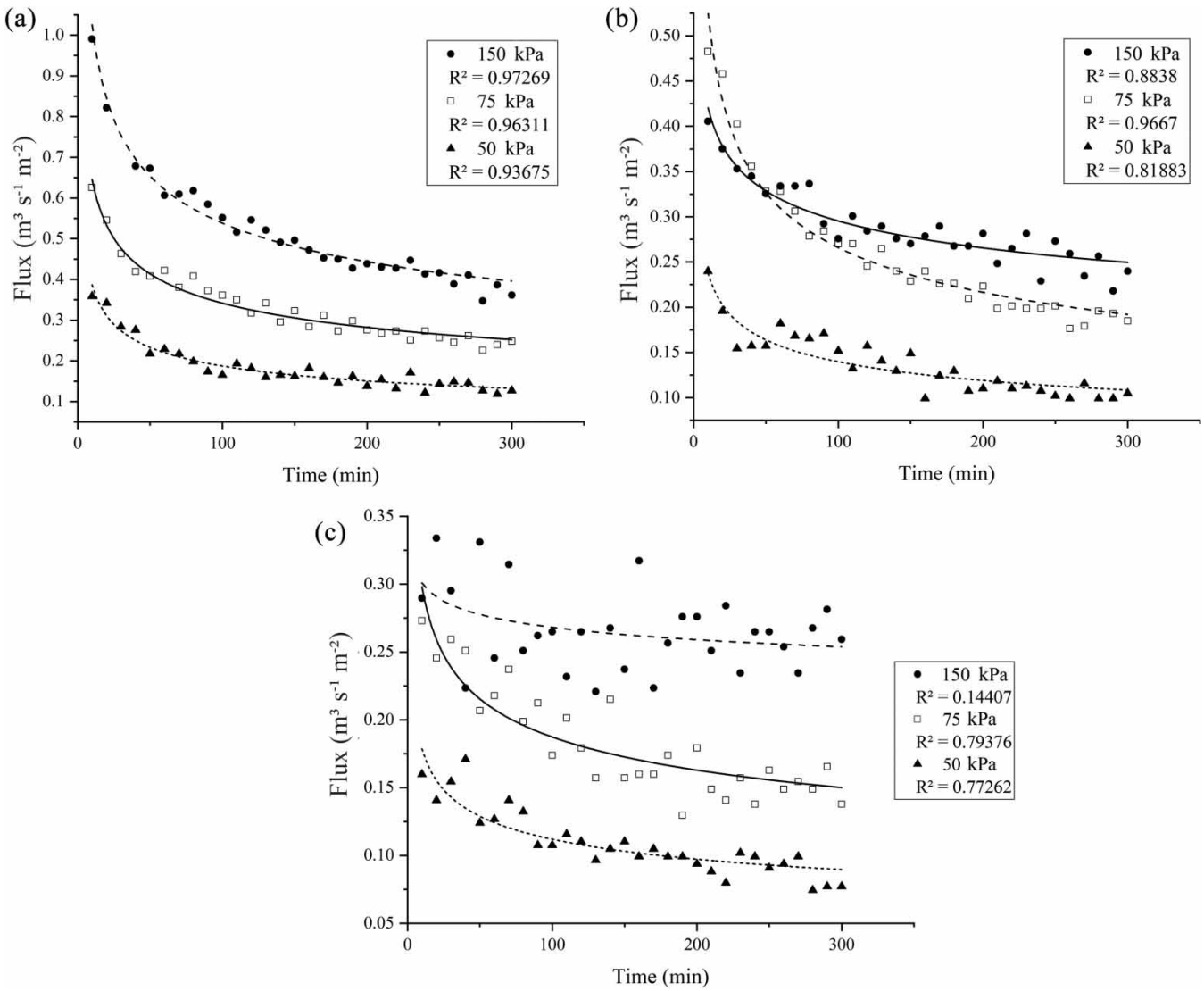

Figure 6 | Porous pipe flux variation as a function of time for the first (a), second (b), and third (c) cumulative tests at pressures of 50, 75, and 150 kPa.

Table 12 shows the mathematical models for the flux as a function of time, fitted to the observed data presented in Figure 5. The intersection of the curves in Figure 6 was explained by Mohammad (1998), who stated that the service pressures for porous pipes are between 80 and 150 kPa and that, at a pressure of 150 kPa, which is high for this type of material, irregular flux behaviour occurs over time. Additionally, when higher pressures are used, stable flux is achieved more quickly. Aboukarima *et al.* (2018) found results similar to those obtained in the present study. After each test, the flux of the porous pipes decreased, even when it was subjected to drying. Other authors have shown that, in addition to the mean

Table 12 | Mathematical models of the flux as a function of time for the tests at pressures of 50, 75, and 150 kPa

Pressure	Test 1	Test 2	Test 3
50 kPa	$q = 0.79854.t^{-0.31476}$	$q = 0.40433.t^{-0.23078}$	$q = 0.28506.t^{-0.20286}$
75 kPa	$q = 1.21919.t^{-0.27616}$	$q = 1.04161.t^{-0.29651}$	$q = 0.47395.t^{-0.20157}$
150 kPa	$q = 1.95259.t^{-0.27972}$	$q = 0.59864.t^{-0.15338}$	$q = 0.33771.t^{-0.05008}$

reduction in flow rates with the use of the material, the application rate stabilizes over time; that is, the outlet flow rate becomes constant (Lomax *et al.* 1986, 1988; Teeluck & Sutton 1998; Donjadee 2012).

It is especially important to highlight that unlike what is observed in Figure 4 and Table 7, which show the effect of the service pressure on the permeability, the flux values increased as the pressure increased, as shown in Figure 6 and Table 13. This trend did not occur for the intrinsic permeability since its values were generally higher at the intermediate pressure of 75 kPa than at 50 and 150 kPa. This result can be explained by the fact that there is a difference between permeability and flux, where flux is related to the characteristics of the fluid and the porous medium and permeability is a property of the porous medium that indicates its ability to facilitate the passage of fluids through its pores (Paula & Campos 2016).

The length of the pipe used could affect the uniformity in the application of water because, as there is a nonuniform distribution of the pores through which the water flux occurs, nonuniform water application might be observed along the pipe length (Patel *et al.* 2011).

Liang *et al.* (2009) found that within the same manufacturing process, pipes with equal wall thickness but with larger diameter have greater water emission uniformity than other pipes. This is due to the larger emission area and greater number of pores in the wall per unit length. In the studies by these authors, only those pipes with the largest diameter (internal diameter of 0.016 m) had acceptable emission uniformity, with coefficient of variation (CV) values below 20% within a pressure range of 45–58 kPa. This result allows us to conclude that in the present study, the variation in the pressure of 150 kPa is not favourable because this pressure affects the pipe diameter and because the application of water at pressures of 50 and 75 kPa exhibited lower variation than that at 150 kPa.

Hydraulic head loss and absolute roughness

Figure 7 shows that the mathematical model that best fits the observed data for the four studied porous pipe samples was an increasing exponential equation, where the head loss values for samples 1 and 2 were close and those for samples 3 and 4 were also close. The R^2 values for all samples, which in this case were greater than 0.95, are also listed; these values confirm that the statistical models can explain the variability in the observed values.

Table 14 shows the mathematical models of the head loss for each sample analysed relative to the fluid flow velocity.

Unlike what was observed by Pinto *et al.* (2014), the friction factor values decreased in samples 2 and 4 with increasing Reynolds number (Figure 8) according to the fitted equation, as defined by the laws of fluid flow. The result of Figure 8 shows that the increase in the internal diameter of the pipes due to the internal pressure affected the obtained values (Rettore *et al.* 2014).

Thus, the mathematical models for the friction factor relative to the Reynolds number for the four samples analysed are as shown in Table 15.

Figure 9 shows the representations of the same mathematical models of Figure 8 based on the Moody diagram. The characterizations given by the diagram can be observed; for example, the transition flow regime relative to the trajectory was observed for all cases. Proving the results obtained, the curves for the four samples show turbulent flow; in addition, the relative roughness values can be observed in the diagram. Furthermore, the analysis of Figure 9 shows that the pipe samples have different roughnesses; however, all analysed samples have a high roughness value compared to other types of materials used in the manufacture of pipes.

Boxplots of the friction factors obtained for the tests performed are shown in Figure 10.

Table 13 | Mathematical models of the flux as a function of time for the first, second, and third cumulative tests at pressures of 50, 75, and 150 kPa

Test	50 kPa	75 kPa	150 kPa
1	$q = 0.79854.t^{-0.31476}$	$q = 1.21919.t^{-0.27616}$	$q = 1.95259.t^{-0.27972}$
2	$q = 0.40433.t^{-0.23078}$	$q = 1.04161.t^{-0.29651}$	$q = 0.59864.t^{-0.15338}$
3	$q = 0.28506.t^{-0.20286}$	$q = 0.47395.t^{-0.20157}$	$q = 0.33771.t^{-0.05008}$

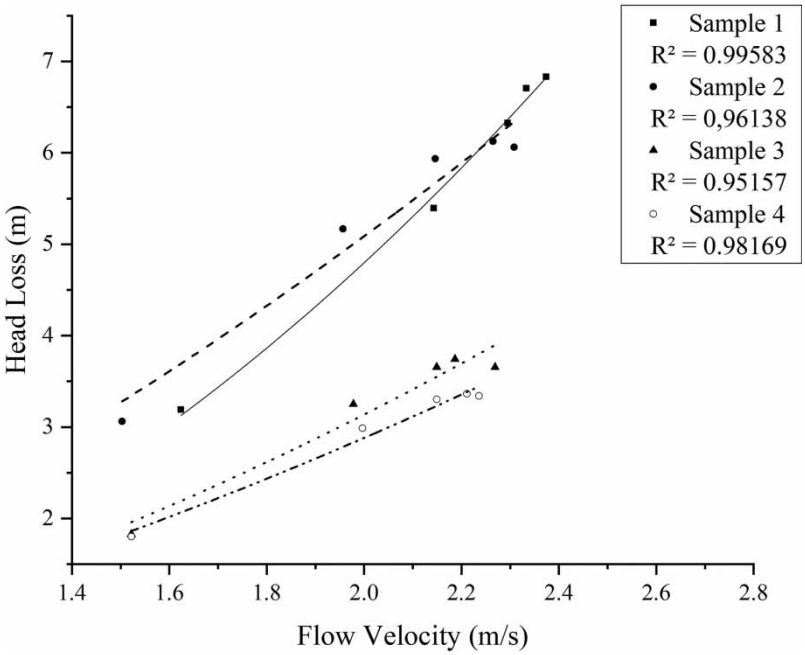

Figure 7 | Head loss as a function of the fluid velocity for four samples from the same batch.

Table 14 | Mathematical models of the head loss as a function of the fluid velocity for four porous pipe samples from the same batch

Sample	Equation
1	$h_f = 1.154.v^{2.05521}$
2	$h_f = 1.75301.v^{1.53697}$
3	$h_f = 0.95131.v^{1.72131}$
4	$h_f = 0.95249.v^{1.5971}$

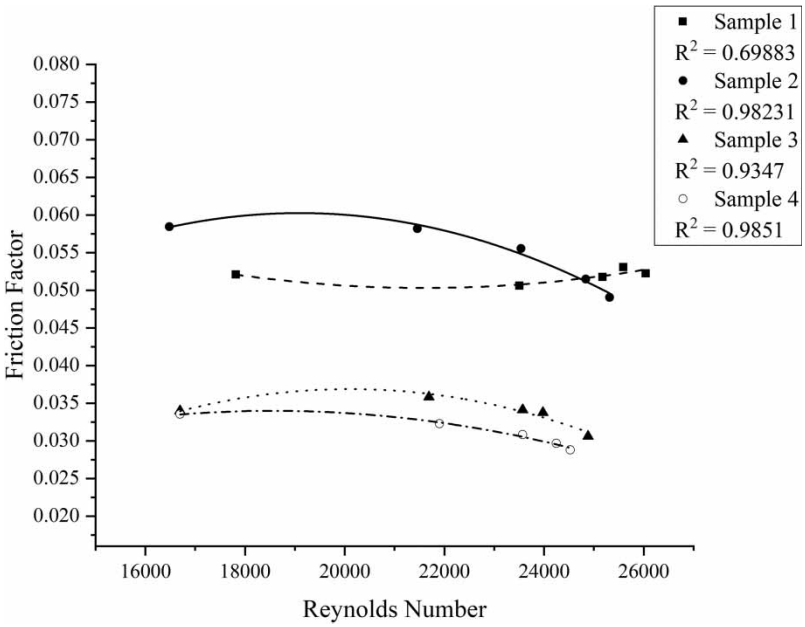

Figure 8 | Variation in the friction factor of the porous pipes relative to the Reynolds number for each sample.

Table 15 | Mathematical models for the friction factor as a function of the Reynolds number for four porous pipe samples from the same batch

Sample	Equation
1	$f = 0.10837 - (5.37726 \cdot 10^{-6})Re + (1.245 \cdot 10^{-10})Re^2$
2	$f = -0.04004 + (1.05051 \cdot 10^{-5})Re - (2.75084 \cdot 10^{-10})Re^2$
3	$f = -0.06466 + (1.00994 \cdot 10^{-5})Re - (2.51141 \cdot 10^{-10})Re^2$
4	$f = -0.01341 + (5.10949 \cdot 10^{-6})Re - (1.3769 \cdot 10^{-10})Re^2$

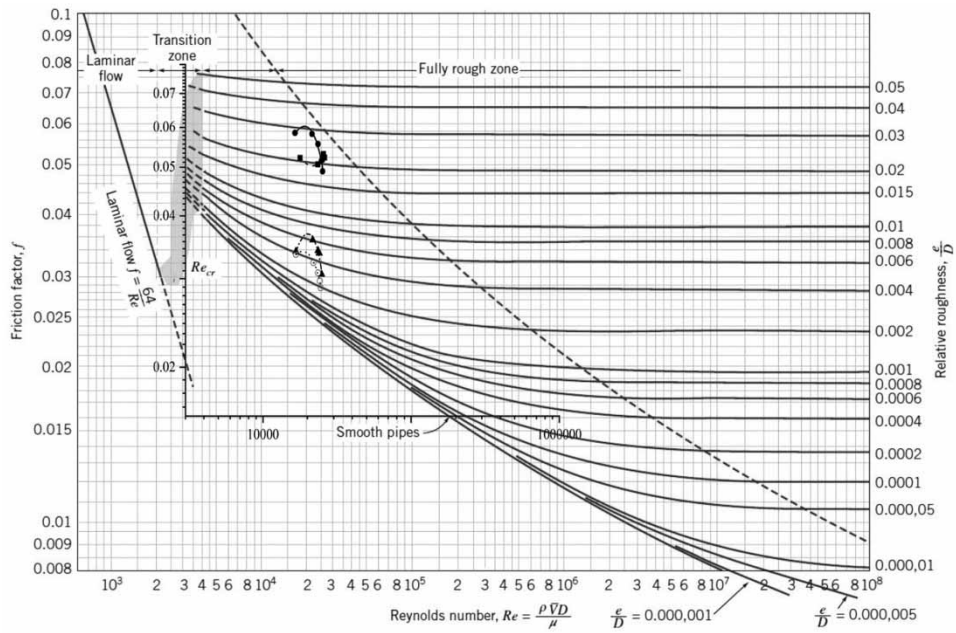

Figure 9 | Variation in the friction factor of the porous pipes relative to the Reynolds number for each sample represented in the Moody diagram. Source: Adapted from Fox *et al.* (2011).

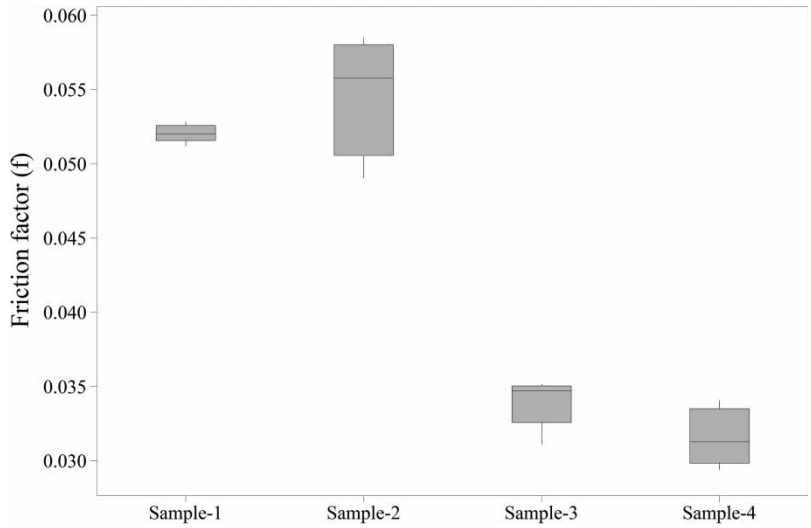

Figure 10 | Boxplots of the friction factor values obtained for the studied porous pipe samples.

Table 16 | Multiple comparisons between pairs of samples given by Tukey's test

Comparison between samples	F
2 vs 4	4.914*
2 vs 3	3.477^{ns}
2 vs 1	0.832^{ns}
1 vs 4	4.082*
1 vs 3	2.646^{ns}
3 vs 4	1.436^{ns}

*Significant difference at the 5% probability level ($p < 0.05$) according to Tukey's test.

The comparison given by Figure 10 within each treatment shows that the friction factor values for sample 1 were close to the median value; thus, the friction factors within this treatment had less variability. In turn, sample 2 had greater data variability, and most of the values found were below the median, which indicated greater variability within the same sample.

Similar to sample 2, there was a higher concentration of values below the third quartile for sample 3, which indicated greater variability in the friction factor for these samples. For sample 4, the greatest concentration of data was above the median. In addition, the median value for samples 2 and 3 was more distant than the minimum value, which showed that there was great variability in the values obtained for the friction factor within the same sample. The medians of samples 1 and 2 were close, as were those of samples 3 and 4. These results showed that the friction factor values obtained for each of the samples were similar between pairs, as revealed in Table 16. Hence, there was variation in the value of the friction factor for each sample analysed even within the same batch.

Because the differences in the median values between the treatment groups were greater than expected, they were statistically significant. The variables were assumed to follow a normal distribution, and a normality test presented a *p*-value of 0.592, i.e., greater than 5%. To compare the samples, Tukey's test was performed using the pairwise multiple comparison procedure. This test showed that there was variation between samples 1 and 4 and between samples 2 and 4 at the 5% significance level in the analysis of the friction factor. There were no significant differences between samples 1 and 2 or between samples 3 and 1. The same analysis was applied for the roughness; the normal distribution yielded a *p*-value of 0.054, and the results of multiple comparison analyses were statistically equal to those of the friction factor.

As demonstrated in studies by Rettore Neto *et al.* (2014), Rettore Neto *et al.* (2014), and Wałowski (2017), there is variation in the characteristics of porous pipe from different batches as a result of the manufacturing process, which causes non-uniformity in the material and consequently changes in the hydraulic characteristics. In this study, it was shown that there is variation even within the same batch, causing non-uniformity in the application of water.

CONCLUSIONS

Porous piping shows variations in intrinsic permeability and flux over time, and this variation depends on the inlet service pressure. The irregular release of water through the pipes occurs over time; however, the variation decreases over time and with the number of tests; that is, irrigation events, and the application of water becomes constant (stable flux).

Therefore, a stable flux can be defined, which allows one to determine the time at which the application of water becomes continuous. This determination can also be used as a reference for the calculation and management of regular situations regarding the use of porous pipes.

There is variability in the friction factor and roughness in each sample, especially compared to each other, indicating variability in the production process within the same batch, which affects the hydraulic behaviour of the pipes.

ACKNOWLEDGEMENTS

The authors thank the Coordenação de Aperfeiçoamento de Pessoal de Nível Superior (CAPES) for funding this research by providing scholarship grant to the first author (no grant number is provided).

DATA AVAILABILITY STATEMENT

All relevant data are included in the paper or its Supplementary Information.

REFERENCES

Aboukarima, A. M., Al-Sulaiman, M. A. & El Marazky, M. S. A. 2018 Effect of sodium adsorption ratio and electric conductivity of the applied water on infiltration in a sandy-loam soil. *Water SA* **44** (1), 105–110. https://doi.org/10.4314/wsa.v44i1.12.

Alam, M. 1995 *Leaky Tubing for Subsurface Irrigation*. AGRIS. Available form: https://agris.fao.org/agris-search/search.do?recordID = US9511216 (accessed 15 April 2020).

Azevedo Netto, J. M. & Fernandez y Fernandez, M. 2015 *Manual de Hidráulica*, 9th edn.. Editor Blücher, São Paulo.

Bradley, G. L., Chang, P. C. & Mckenna, G. B. 2001 Rubber modeling using uniaxial test data. *Journal of Applied Polymer Science* **81** (4), 837–848. https://doi.org/10.1002/app.1503.

Cai, Y., Zhao, X., Wu, P., Zhang, L., Zhu, D. & Chen, J. 2018 Effect of soil texture on water movement of porous ceramic emitters: a simulation study. *Water* **11** (1), 22. https://doi.org/10.3390/w11010022.

Casimiro, J. 2011 *Modifications de surfaces de materiaux polymers pour des visées antibacteriennes*. Université Paris Sud. Available form: https://tel.archives-ouvertes.fr/tel-00651058 (accessed 10 March 2020).

Donjadee, S. 2012 Water application technology with porous pipe. *Journal of the Thai Society of Agricultural Engineering*, 34–42. https://li01.tci-thaijo.org/index.php/TSAEJ/article/view/63928/52458.

Fang, Y., Zhan, M. & Wang, Y. 2000 The status of recycling of waste rubber. *Materials and Design* **22** (2), 123–127. https://doi.org/10.1016/s0261-3069(00)00052-2.

Fox, R. W., Pritchard, P. J. & Leylegian, J. C. 2011 *Introduction to Fluid Mechanics*, 8th edn.. John Wiley & Sons Inc.; John Wiley, New Jersey.

Janani, A., Sohrabi, T. & Dehghanisanji, H. 2011 Pressure variation impact on discharge characteristics of porous pipes. http://wg-on-farm.icidonline.org/micro_irrigation_tehran.pdf#page=284 (acessed 10 June 2021).

Kanda, E. K., Mabhaudhi, T. & Senzanje, A. 2018 Hydraulic and clogging characteristics of Moistube irrigation as influenced by water quality. *Journal of Water Supply: Research and Technology - Aqua* **67** (5), 438–446. https://doi.org/10.2166/aqua.2018.166

Kang, Y. 2000 Effect of operating pressures on microirrigation uniformity. *Irrigation Science* **20** (1), 23–27. https://doi.org/10.1007/s002710000024.

Kostiakov, A. N. 1932 On the dynamics of the coefficient of water percolation in soils and the necessity of studying it from the dynamic point of view for the purposes of amelioration. *Transactions of 6th Committee International Society of Soil Science*, 17–21. http://ci.nii.ac.jp/naid/10011005232/en/.

Kowalska, E., Wielgosz, Z. & Pelka, J. 2002 Use of post-life waste and production waste in thermoplastic polymer compositions. *Polymers and Polymer Composites* **10** (1), 83–92. https://doi.org/10.1177/096739110201000107.

Liang, H., Liu, Z., Shu, Q. & Yin, G. 2009 Effects of operating pressure on the discharge characteristics of porous pipes as micro-irrigation laterals. *Transactions of the Chinese Society of Agricultural Engineering* **25** (1), 1–5. https://www.cabdirect.org/cabdirect/abstract/20093149742.

Lomax, K. M., Wood, J. D. & Guacelli, F. S. 1986 *Particles Influence Hydraulics of Porous Tubing*. American Society of Agricultural Engineers. Microfiche Collection (USA). Available form: https://agris.fao.org/agris-search/search.do?recordID = US875845188 (accessed 08 March 2020).

Lomax, K. M., Wood, J. D. & Guacelli, F. S. 1988 Emission characteristics of porous tubing. *Agricultural Water Management* **15** (2), 197–204. https://doi.org/10.1016/0378-3774(88)90112-6.

Lyu, F., Zhang, M., Qu, Y., Gao, J., Jia, X., Hao, X. & Wu, M. 2016 Estimation of reversed flow in long pipeline based on axial vibration model of dense paste. *Shock and Vibration* **2016**, 1–7. https://doi.org/10.1155/2016/6198793

Mohammad, F. S. 1998 Porous-tube subsurface irrigation. *Journal of Agricultural and Marine Sciences [JAMS]* **3** (2), 49–57. https://journals.squ.edu.om/index.php/jams/article/view/533.

Patel, G. R., Ghaghada, R. H. & Chalodia, A. L. 2011 Hydraulics performance evaluation of porous pipe (Subsurface) irrigation system. *International Journal of Agricultural Engineering* **4** (2), 156–159.

Paula, T. L. F. & Campos, J. E. G. 2016 Aquíferos com fluxos controlados simultaneamente por porosidade intergranular e planar: Aplicação a rochas metassedimentares do Alto Paraguai, MT. *Revista Brasileira de Recursos Hídricos* **21** (1), 11–24. https://doi.org/10.21168/rbrh.v21n1.p11-24.

Pinto, M. F., Camargo, A. P., Rettore Neto, O. & Frizzone, J. A. 2014. Caracterização hidráulica de tubos porosos oriundos de pneus reciclados utilizados em irrigação subsuperficial (Hydraulic characterization of porous pipes made of recycled automobile tires used in subsurface irrigation). *Revista Brasileira de Engenharia Agrícola e Ambiental* **18** (11), 1095-1101. https://doi.org/10.1590/1807-1929/agriambi.v18n11p1095-1101

Ren, C., Zhao, Y., Wang, J., &Bai, D., Zhao, X. & Tian, J. 2017 Lateral hydraulic performance of subsurface drip irrigation based on spatial variability of soil: Simulation. *Agricultural Water Management* **193**. https://doi.org/10.1016/j.agwat.2017.08.014.

Rettore Neto, O. & Frizzone, J. A. 2014 Hydraulic characterization of porous pipes made of recycled automobile tires used in subsurface irrigation. *Revista Brasileira de Engenharia Agricola e Ambiental* **18** (11), 1095–1101. https://doi.org/10.1590/1807-1929/agriambi.v18n11p1095-1101.

Rettore Neto, O., Botrel, T. A., Frizzone, J. A. & Camargo, A. P. 2014 Method for determining friction head loss along elastic pipes. *Irrigation Science* **32** (5), 329–339. https://doi.org/10.1007/s00271-014-0431-7.

Sant'Anna, L. T., Machado, R. T. M. & Brito, M. J. 2015 A Logística Reversa de Resíduos Eletroeletrônicos no Brasil e no Mundo: O Desafio da Desarticulação dos Atores (Reverse Logistics of Electronic Waste in Brazil and in The World: The Challenge of Dismantling the Actors). *Sustentabilidade em debate* **6** (2), 88–105. https://doi.org/10.18472/SustDeb.v6n2.2015.15522

Shahzad, M., Kamran, A., Siddiqui, M. Z. & Farhan, M. 2015 Mechanical characterization and FE modelling of a hyperelastic material. *Materials Research* **18** (5), 918–924. https://doi.org/10.1590/1516-1439.320414.

Shu, Q., Liu, Z., Wang, Z. & Liang, H. 2007 Simulation of the soil wetting shape under porous pipe sub-irrigation using dimensional analysis. *Irrigation and Drainage* **56** (4), 389–398. https://doi.org/10.1002/ird.290.

Teeluck, M. & Sutton, B. G. 1998 Discharge characteristics of a porous pipe microirrigation lateral. *Agricultural Water Management* **38** (2), 123–134. https://doi.org/10.1016/S0378-3774(98)00060-2.

Tripathi, V., Rajput, T. B. S., Patel, N. & Lata, L. 2011 Hydraulic performance of drip irrigation system with municipal wastewater. *Journal of Agricultural Engineering* **48** (2), 15–22.

Wałowski, G. 2017 Assessment of gas permeability coefficient of porous materials. *Journal of Sustainable Mining* **16** (2), 55–65. https://doi.org/10.1016/j.jsm.2017.08.001.

Zhang, L., Wu, P., Zhu, D. & Zheng, C. 2017 Effect of pulsating pressure on labyrinth emitter clogging. *Irrigation Science* **35**, 267–274.

First received 13 June 2021; accepted in revised form 15 August 2021. Available online 25 August 2021